Advanced Materials Research Vol. 1018 (2014) pp 373-380
© (2014) Trans Tech Publications, Switzerland
doi:10.4028/www.scientific.net/AMR.1018.373

Evaluating Mobile Machine Tool Dynamics by Substructure Synthesis

Mohit Law[1,a], Hendrik Rentzsch[1,b] and Steffen Ihlenfeldt[1,c]

[1]Fraunhofer Institute for Machine Tools and Forming Technology IWU, 09126 Chemnitz, Germany*

[a]mohit.law@iwu.fraunhofer.de, [b]hendrik.rentzsch@iwu.fraunhofer.de,
[c]steffen.ihlenfeldt@iwu.fraunhofer.de

Keywords: Dynamics, Synthesis, Mobile machine tool

Abstract. Mobile machining solutions use autonomous machining units that can be transported to different part locations, making possible easy maintenance and repair of large industrial equipment. Every new part and location results in different boundary conditions for the mobile machine tool-part system, influencing the dynamics of the combined system and necessitating different strategies for part/machine referencing and clamping. To facilitate efficient mutability and modularity in mobile machining solutions, this paper presents a dynamic substructuring strategy that combines the response characteristics of the mobile machine unit with that of two different simulated base models under varying levels of contact stiffness and damping to obtain the synthesized mobile machine tool dynamic response. Numerical verification of the approach is provided. The framework presented can also combine measured response of parts for which models may not be available *a priori*. Methods presented provide experimental guidelines for establishing strategies for part/machine referencing and planning of machining strategies based on the evaluated dynamics.

Introduction

Recent growth in the transport, energy, aeronautical and naval industries has led to increased requirements for large parts manufacturing and their maintenance [1]. Conventional approaches to maintain and repair these large parts by taking the equipment to specialized workshops are not always viable due to the high transportation and associated energy costs, high risk of damage to the part(s) and the challenges with long downtimes for the entire plant. In this context, innovative solutions such as the use of transportable mobile machine tools offer the advantage of moving the machine to the part location, making possible small compact machine solutions with lesser transport and energy costs [2]. The basic idea is to use autonomous machining units that can be transported to part location and which are placed locally at the part.

Every new part and location to which the mobile machine is moved results in different boundary conditions for the machine-part system, influencing the dynamics of the combined system and necessitating different strategies for part/machine referencing and clamping. Machines can be directly or indirectly coupled to the part through another base/frame as shown in Fig. 1. In the case of direct coupling, the part acts as sort of a machine base and its stiffness plays a crucial role in the overall response of the system, whereas the indirect coupling case requires a modular connection element whose stiffness may similarly influence the overall response of the system. In either case, the tool centre point dynamics and the machining strategy to be employed are significantly influenced by the part, the coupling type and the interface characteristics at the point of coupling.

Characterizing these varying influences at the preparatory stage has been largely unaddressed in the available literature, partly because analyses that rely on large order finite element (FE) machine models makes investigations under changing conditions computationally expensive and prohibitive. Since simulation based investigations often provide useful guidelines for experiments, lack of the former has made difficult the effective utilization of mobile machine solutions in practice. Hence, the main focus of this paper is to formulate an approach that allows efficient investigation of mobile machine tool dynamics under varying base/part/contact characteristics, with the aim of establishing experimental guidelines for part/machine referencing and for planning of machining strategies.

Figure 1: Two examples of mobile machines tools. Mobile machine directly mounted onto the part (*left*) [1]; Mobile machine connected to an independent base frame (*right*)

We employ a dynamic substructuring approach in which the structural dynamics of large and/or complex structures is determined using measurements and/or models for individual components [3]. Substructural analysis involves representing individual components by their spatial mass, stiffness and damping, or by their modal data using receptances, i.e. frequency response functions (FRFs). The receptance coupling substructure analysis (RCSA) method is preferred in the present case since component FRFs are only required at the coupling locations between the machine and the part/base as well as at any point where the assembly response is to be predicted.

Earlier RCSA investigations in [4] and [5] reported substructuring results for the simple case of two substructures in contact at a single location, e.g. tool and tool-holder connection, and are not directly applicable to the present case in which the machine may be connected to the part/base at multiple locations. Hence, the multiple point receptance coupling formulations of Schmitz and Duncan [6] are extended presently to predict mobile machine dynamics under varying influences.

In this paper, the dynamic substructuring approach is formulated for a representative example of a pentapod type parallel kinematic mobile machine tool shown in Fig. 1 (*right*). Synthesized tool point dynamics are formulated using virtual FE models of the machine/base available elsewhere in [7], with the possibility of combining machine model response with measured response for different base(s)/part(s) as desired. FRFs for each component(s) investigated need be obtained only once from single runs of their respective substructural FE models, with synthesis under varying base/part/contact characteristics taking place outside the FE environment. This makes for efficient investigations of tool centre point dynamics while dramatically reducing the computational effort that was earlier required with large order FE models for the composite machine-base/part system.

Multiple Point Receptance Coupling Substructural Analysis

The mobile machine in contact with the base at multiple points is shown schematically in Fig. 2.

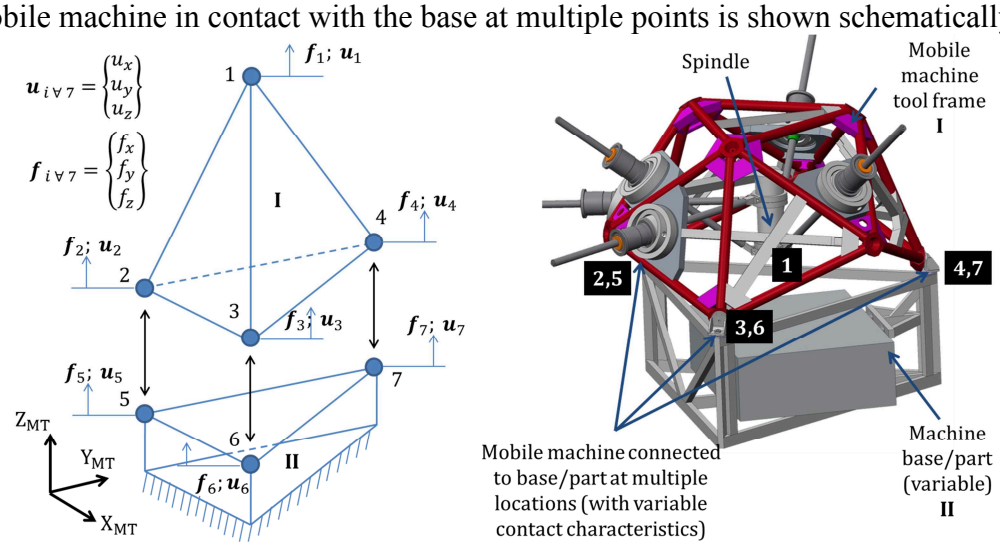

Figure 2: Multiple point RCSA representation (*left*); and, the machine CAD model (*right*)

Response after assembly is desired at location 1 within Fig. 2, i.e. the free-end of substructure I that corresponds to the tool centre point of the mobile machine tool. Locations 2-4 correspond to the mounting locations of the mobile platform which are to be connected to locations 5-7 on substructure II which correspond to a machine base/part. Each of the contacting interfaces on each of the coupling surfaces is approximated by a single node in the FE environment to ease the process of dynamic substructuring. Each of the coupling nodes (locations) has three translational degrees of freedom, making the component receptances for any node in compact matrix form to be:

$$\begin{Bmatrix} u_x \\ u_y \\ u_z \end{Bmatrix}_i = \begin{bmatrix} h_{xx} & h_{xy} & h_{xz} \\ h_{yx} & h_{yy} & h_{yz} \\ h_{zx} & h_{zy} & h_{zz} \end{bmatrix}_{ij} \begin{Bmatrix} f_x \\ f_y \\ f_z \end{Bmatrix}_j \tag{1}$$

wherein h represents the displacement-to-force receptance; i and j are the respective measurement and excitation locations. Eq. 1 may be rewritten in its generalized form as:

$$\boldsymbol{u}_i = \boldsymbol{R}_{ij}\boldsymbol{f}_j \tag{2}$$

where $\boldsymbol{R}_{ij}$ is the generalized receptance matrix describing translational component behaviour and $\boldsymbol{u}_i$ and $\boldsymbol{f}_j$ are the corresponding generalized displacement and force vectors. The component level receptances (both direct and cross) for each of the substructures may be defined in compact form as:

$$\begin{aligned} \boldsymbol{u}_1 &= \boldsymbol{R}_{11}\boldsymbol{f}_1 + \boldsymbol{R}_{12}\boldsymbol{f}_2 + \boldsymbol{R}_{13}\boldsymbol{f}_3 + \boldsymbol{R}_{14}\boldsymbol{f}_4 \\ \boldsymbol{u}_2 &= \boldsymbol{R}_{22}\boldsymbol{f}_2 + \boldsymbol{R}_{21}\boldsymbol{f}_1 + \boldsymbol{R}_{23}\boldsymbol{f}_3 + \boldsymbol{R}_{24}\boldsymbol{f}_4 \\ \boldsymbol{u}_3 &= \boldsymbol{R}_{33}\boldsymbol{f}_3 + \boldsymbol{R}_{31}\boldsymbol{f}_1 + \boldsymbol{R}_{32}\boldsymbol{f}_2 + \boldsymbol{R}_{34}\boldsymbol{f}_4 \\ \boldsymbol{u}_4 &= \boldsymbol{R}_{44}\boldsymbol{f}_4 + \boldsymbol{R}_{41}\boldsymbol{f}_1 + \boldsymbol{R}_{42}\boldsymbol{f}_2 + \boldsymbol{R}_{43}\boldsymbol{f}_3 \end{aligned} \tag{3}$$

for substructure I. Similarly, the component level receptances for substructure II are:

$$\begin{aligned} \boldsymbol{u}_5 &= \boldsymbol{R}_{55}\boldsymbol{f}_5 + \boldsymbol{R}_{56}\boldsymbol{f}_6 + \boldsymbol{R}_{57}\boldsymbol{f}_7 \\ \boldsymbol{u}_6 &= \boldsymbol{R}_{66}\boldsymbol{f}_6 + \boldsymbol{R}_{67}\boldsymbol{f}_7 + \boldsymbol{R}_{65}\boldsymbol{f}_5 \\ \boldsymbol{u}_7 &= \boldsymbol{R}_{77}\boldsymbol{f}_7 + \boldsymbol{R}_{76}\boldsymbol{f}_6 + \boldsymbol{R}_{75}\boldsymbol{f}_5. \end{aligned} \tag{4}$$

Equilibrium conditions for a force $\boldsymbol{F}_1$ applied at location 1 in the assembled configuration are:

$$\boldsymbol{F}_1 = \boldsymbol{f}_1;\ \boldsymbol{f}_2 + \boldsymbol{f}_5 = 0;\ \boldsymbol{f}_3 + \boldsymbol{f}_6 = 0\ and\ \boldsymbol{f}_4 + \boldsymbol{f}_7 = 0. \tag{5}$$

Interface compatibility conditions for a flexible contact with a viscous damping model are [6]:

$$\boldsymbol{K}(\boldsymbol{u}_5 - \boldsymbol{u}_2) = \boldsymbol{f}_5;\ \boldsymbol{K}(\boldsymbol{u}_6 - \boldsymbol{u}_3) = \boldsymbol{f}_6\ and\ \boldsymbol{K}(\boldsymbol{u}_7 - \boldsymbol{u}_4) = \boldsymbol{f}_7, \tag{6}$$

wherein the complex stiffness matrix for constant levels of stiffness, $k_{x,y,z}$ and damping, $c_{x,y,z}$ is:

$$\boldsymbol{K} = \begin{bmatrix} k_x + i\omega c_x & 0 & 0 \\ 0 & k_y + i\omega c_y & 0 \\ 0 & 0 & k_z + i\omega c_z \end{bmatrix}. \tag{7}$$

Although a single $\boldsymbol{K}$ matrix is employed in Eq. 6, each coupling location and/or direction could have a different stiffness and/or damping. Describing the damping using the modal damping ratio ζ, the coefficient becomes: $c = 2\zeta\sqrt{km}$; wherein m, the mass of the joint, is assumed to be unity.

With brevity the desired assembled tool centre point response matrix $\boldsymbol{G}_{11}$, which is synthesized from the individual substructural receptances, can be shown to be:

$$\boldsymbol{G}_{11} = \boldsymbol{R}_{11} + \boldsymbol{R}_{12}\frac{\boldsymbol{f}_2}{\boldsymbol{F}_1} + \boldsymbol{R}_{13}\frac{\boldsymbol{f}_3}{\boldsymbol{F}_1} + \boldsymbol{R}_{14}\frac{\boldsymbol{f}_4}{\boldsymbol{F}_1}, \tag{8}$$

wherein the following ratios are desired: $\boldsymbol{f}_2/\boldsymbol{F}_1$, $\boldsymbol{f}_3/\boldsymbol{F}_1$ and $\boldsymbol{f}_4/\boldsymbol{F}_1$. These ratios may be obtained by first substituting the component receptances in Eq. 3-4 into the compatibility of Eq. 6 and eliminating $\boldsymbol{f}_5, \boldsymbol{f}_6, and\ \boldsymbol{f}_7$ from the resultant expressions by substituting relations from the equilibrium conditions of Eq. 5. The three desired ratios in compact form reduce to:

$$\begin{Bmatrix} \boldsymbol{f}_2 \\ \boldsymbol{f}_3 \\ \boldsymbol{f}_4 \end{Bmatrix} \begin{Bmatrix} \boldsymbol{F}_1 \\ \boldsymbol{F}_1 \\ \boldsymbol{F}_1 \end{Bmatrix}^{-1} = \begin{bmatrix} \boldsymbol{R}_{22} + \boldsymbol{R}_{55} + \boldsymbol{K}^{-1} & \boldsymbol{R}_{23} + \boldsymbol{R}_{56} & \boldsymbol{R}_{24} + \boldsymbol{R}_{57} \\ \boldsymbol{R}_{32} + \boldsymbol{R}_{65} & \boldsymbol{R}_{33} + \boldsymbol{R}_{66} + \boldsymbol{K}^{-1} & \boldsymbol{R}_{34} + \boldsymbol{R}_{67} \\ \boldsymbol{R}_{42} + \boldsymbol{R}_{75} & \boldsymbol{R}_{43} + \boldsymbol{R}_{76} & \boldsymbol{R}_{44} + \boldsymbol{R}_{77} + \boldsymbol{K}^{-1} \end{bmatrix}^{-1} \begin{bmatrix} -\boldsymbol{R}_{21} \\ -\boldsymbol{R}_{31} \\ -\boldsymbol{R}_{41} \end{bmatrix} = [\boldsymbol{A}] \tag{9}$$

wherein $[\boldsymbol{A}]$ is 9×3, or $3n \times 3 \times N$ matrix (N is the number of points in the frequency vector, ω, and n corresponds to the number of connection points). The matrix size is 9×3 because $\boldsymbol{R}_{ij}$ is a 3×3 matrix. The first three rows of $[\boldsymbol{A}]$ give $\boldsymbol{f}_2/\boldsymbol{F}_1$, the next three rows give $\boldsymbol{f}_3/\boldsymbol{F}_1$ and the final three rows give $\boldsymbol{f}_4/\boldsymbol{F}_1$. By substituting these ratios into Eq. 8, the desired receptance matrix at the tool centre point in all machine tool principal directions can be computed.

Each time the mobile machine is mounted on a different base/part with different interface characteristics, a new set of component receptances are constructed from a new FE model or from measurements with relevant changes to contact characteristics, allowing for efficient investigations.

Substructural Response Characteristics

For better understanding the substructural characteristics and their interaction, direct and cross responses of both substructures are compared in this section. For each of the receptances considered herein, if otherwise not stated explicitly, a uniform damping of the level of $\zeta = 0.04$ is assumed for all structural modes belonging to the base and a level of $\zeta = 0.05$ is assumed for all structural modes belonging to the machine. Response comparisons are limited up to 400 Hz, i.e. the range corresponding to global substructural modes. SI base units were used for all calculation examples.

Machine Tool Response. Direct and free-free response of the mobile machine for all directions at the tool centre point and at a representative coupling location is compared in Fig. 3. In the case of the direct tool point response, the Z directional response appears stiffer than the X and Y directions, except for one mode, whereas response at the representative coupling location 2 appears to be symmetric in all directions and is almost as flexible as the tool point response.

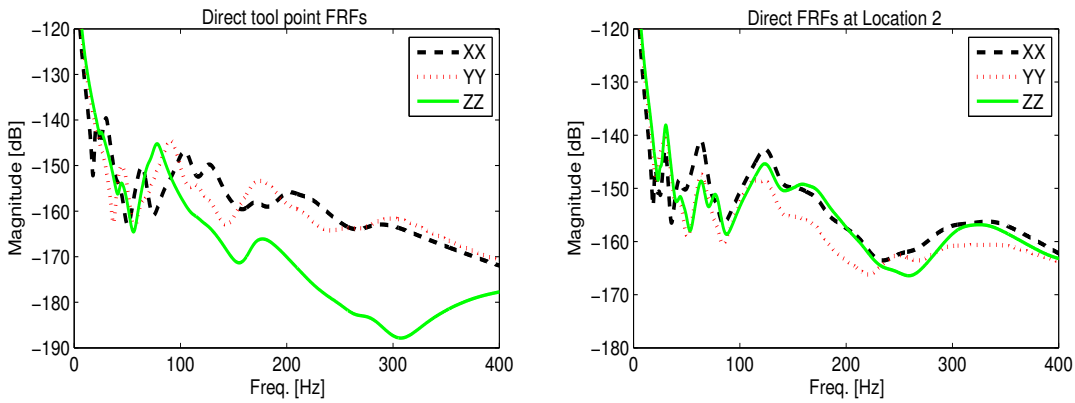

Figure 3: Free-free direct responses for substructure I. Response at tool centre point (*left*); Response at location 2 (*right*)

Fig. 4 compares the cross FRFs between the tool and the coupling location 2 as well as between coupling locations 2 and 4. From the frequency spectrum in either case it appears that different modes for different directions become dominant at different frequencies. There also appears some significant cross-talk between the two locations and this is expected to influence the overall assembled tool point response, as evident from the synthesized formulation in Eq. 8-9.

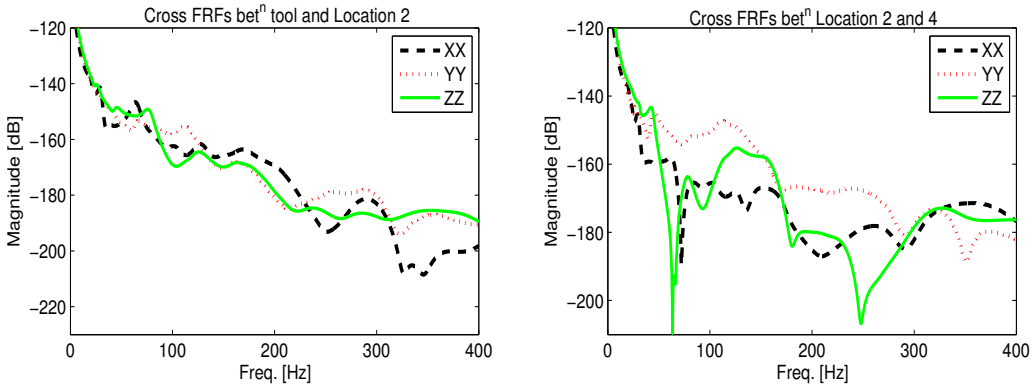

Figure 4: Free-free cross responses for substructure I. Response between tool and coupling location 2 (*left*); Response between locations 2 and 4 (*right*)

Base Response. Direct responses at coupling location 5 and cross response between locations 5 and 7 for the base considered in Fig. 2 are shown in Fig. 5. The Y directional response in either case appears more flexible than the X directional response. The Z directional response is sufficiently stiffer than both the X and Y directions. There appears significant cross-talk between the two different connection locations on the base, and though the base response is stiffer than the machine response there exist several modes which may interact with the machine response when assembled.

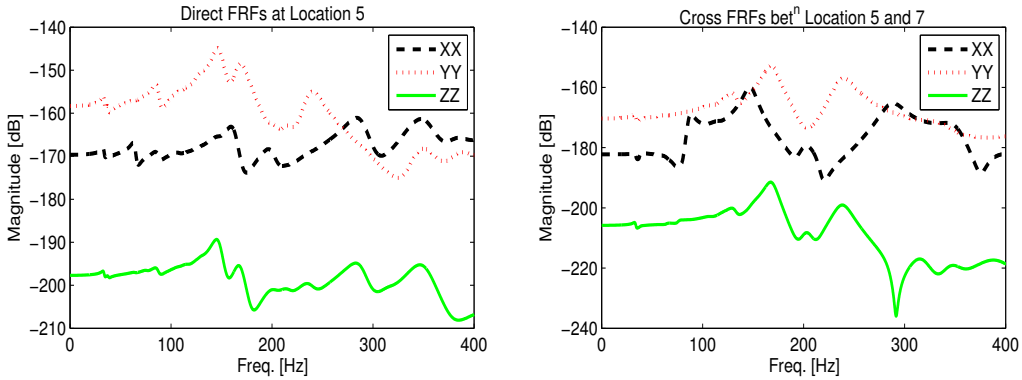

Figure 5: Responses for substructure II. Direct response at coupling location 5 (*left*); Cross response between locations 5 and 7 (*right*)

Assembled Tool Point Response

At first, substructures are assembled to be in rigid contact, i.e. by setting $\boldsymbol{K} = 0$ in Eq. 9, following which influences under changing base/part/contacts are investigated. The effect of mode interactions between the two substructures as well as between different coupling points is evident in assembled tool point results of Fig. 6, which are significantly different than the individual substructural responses in Figs. 3-5. Response seems dominated by the Z directional mode at ~58 Hz, which corresponds to a global machine frame mode for the given configuration. Hence, most of the subsequent discussions for investigations under varying influences are limited to the Z direction.

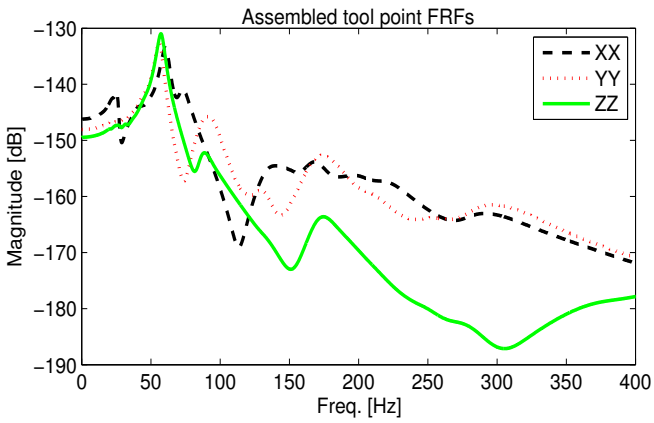

Figure 6: Assembled direct tool centre point response for the machine with base configuration shown in Fig. 2

Investigations under Varying Influences

Influences of variable stiffness and damping at the contacting interfaces on the assembled tool point dynamics are herein investigated, following which changes to tool point dynamics when the mobile machine is connected to an alternate base model is investigated.

Variable Contact Characteristics. Two cases are investigated: variable stiffness for constant level of damping and variable damping for constant stiffness. Stiffness and damping for all directions and all locations is taken to be the same. Stiffness and damping levels are ranged between *low, medium,* and *high*, as: $k_{x,y,z} = 2e6, 1e7,$ and 5e8 N/m and as: $\zeta_{x,y,z} = 0.01$, 0.1, and 0.5.

Variable Stiffness for Constant Damping. Inclusion of springs at the interfaces results in a more flexible contact at the interface than in the rigid case and results in lower frequencies and dynamic stiffness's as observed in the comparisons in Fig. 7. Joint damping for these investigations is assumed constant at $\zeta = 0.1$. A comparison of the joint FRFs (constructed from the joint parameters) in Fig. 7 clearly shows that for higher contact stiffness the joint mode falls outside the frequency range of interest and hence has little effect on the assembled response, making the results for the joint with a *high stiffness* approaching the case of rigid connection. For the *low* and *medium* level of joint stiffness the low-frequency slope of the joint FRF as well as the high-frequency slope of the joint FRF interacts with the assembly response to significantly alter the response of the coupled system in comparison to a rigid/*high* contact stiffness connection.

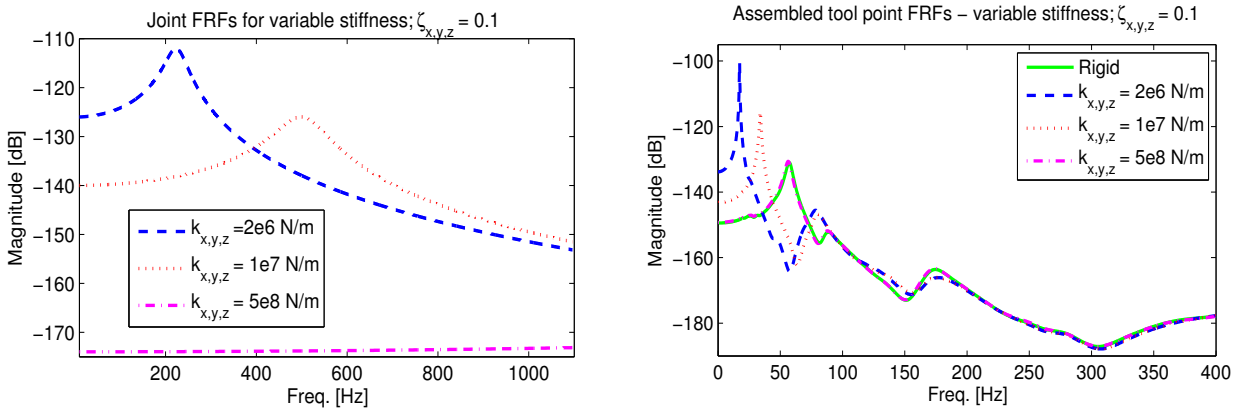

Figure 7: Z directional tool centre point results for variable stiffness and constant damping. Joint FRFs (*left*); Assembled direct tool centre point response (*right*)

Variable Damping for Constant Stiffness. For a constant *medium* level of stiffness and for variable levels of damping, the joint FRFs along with assembled tool point response are compared in Fig. 8. Tool point response comparisons are limited to 100 Hz. Clearly, higher levels of damping lead to a significantly dynamically stiffer system than lower levels, with the slope of the joint's FRF interacting with the assembled system response to increase the dynamic stiffness.

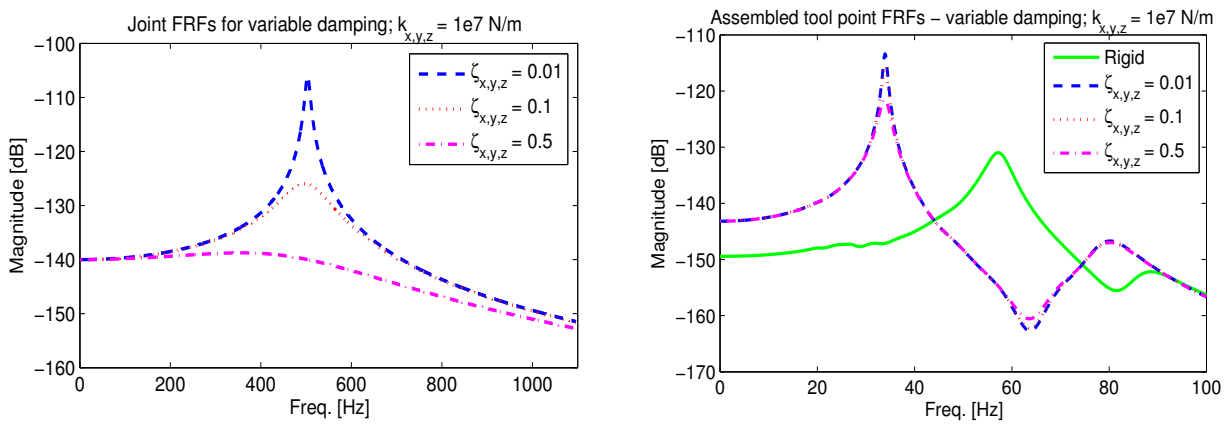

Figure 8: Z directional tool point results for variable damping and constant stiffness. Joint FRFs (*left*); Assembled direct tool point response (*right*)

Influence of Different Machine Base. Influence of changing the base/part onto which the mobile machine is mounted is evaluated by approximating an alternate base/part with a simplified mathematical four degree of freedom (DOF) model, parameters of which are shown in Fig. 9. Mass and stiffness of each the three coupling DOFs are taken to be identical and damping is ignored. Parameters in all three principal directions (X, Y and Z) are assumed to be identical.

The direct response at the connection ends of this base model along with the cross response between two connection DOFs is also shown in Fig. 9. As evident, this base model is significantly more flexible than the response of the original base model discussed in Fig. 5.

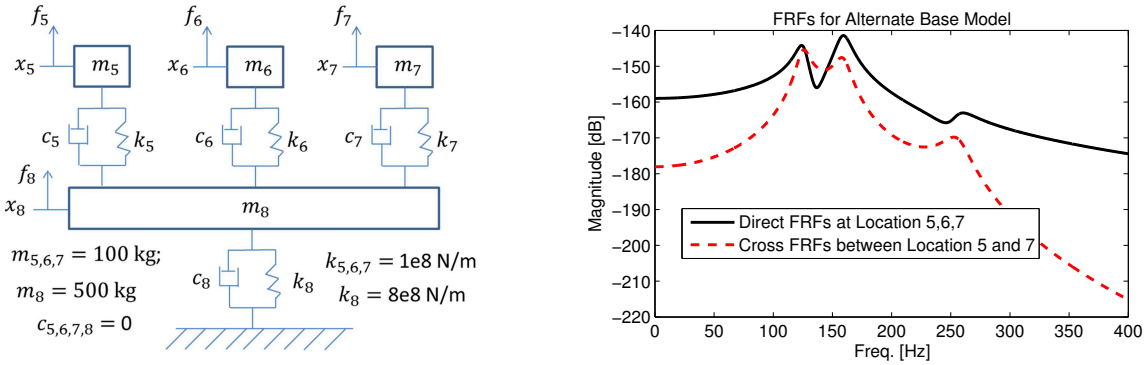

Figure 9: Alternate base/part model (*left*); Direct response at and cross response between coupling locations (*right*). Location numbering is consistent with Fig. 2.

Influence of changing boundary conditions due to change in base models are isolated by assuming the different substructures to be in rigid contact. Assembled tool point response for both base models as well as for the case of connecting the mobile machine directly and rigidly to the ground are shown in Fig. 10. Response comparisons are limited to only the X and Z directions. Since the Z directional response was significantly stiffer than the X and Y directions for the original base model than the alternate base model, assembled response in the Z direction does not change much for when the machine is connected to the ground or to the original base model. Contrastingly, assembled response in the X direction appears to change more when the machine is grounded than between response with either of the base models. Overall, since mobile machine response is more flexible than the either of the base models investigated, its modes dominate the response spectrum.

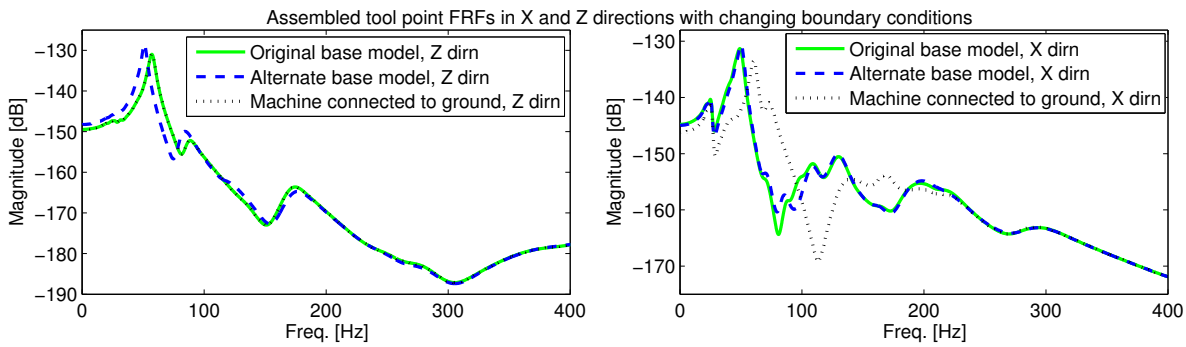

Figure 10: Comparison of the effect of different base models on assembled tool point response

Verification, Limitations and Strengths of the Proposed Approach

Tool point response obtained with the multiple point RCSA approach is compared in Fig. 11 with results obtained for a combined FE model of the machine-base system for the configuration shown in Fig. 2. The RCSA approach quite reasonably captures the trend of the combined response and the slight differences between the two FRFs may partially be attributed to the fact that the three point coupling presently employed may be insufficient to capture the complete modal behaviour of the combined model. It is also possible that a coupling point may well be a nodal location for a particular mode, contributing further to the errors. This remains a limitation of the proposed approach, one that can potentially be overcome by employing more coupling points to more accurately represent the modal properties of the combined system, as proposed in [6].

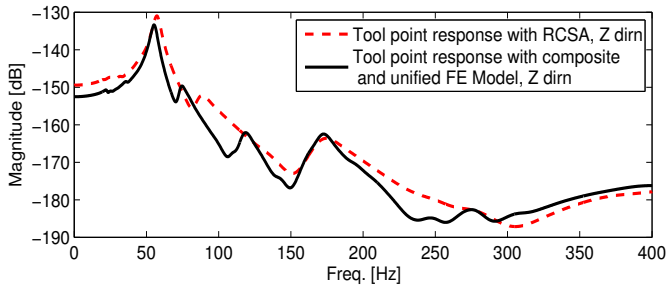

Figure 11: Comparison of tool centre point response with the RCSA approach and results for the combined model from FE. Substructures assumed to be in rigid contact.

The hierarchical dynamic substructuring framework presented above allows efficient investigations under varying influences and also facilitates multi-stage dynamic substructuring, making possible evaluation of situations when the machine is mounted on the part, which in turn may be mounted on another base. Moreover, for the present application, since models for parts may not be available *a priori*, these can be independently measured on location and synthesized with validated machine response as desired, which is thought to be the real strength of the approach.

Conclusions and Outlook

A dynamic substructuring strategy is proposed to evaluate mobile machine tool dynamics under varying influences of changing base/part and contact interface characteristics. Simulation driven investigations with different levels of contact stiffness and damping and with different base models shows the dependence of the tool centre point dynamics under these varying influences. Methods presented provide guidelines for: selection of suitable clamping devices, strategies for part/machine referencing and for planning of machining strategies based on the evaluated dynamics. This results in savings of valuable time and effort by mitigating trial-and-error approaches. As part of the planned future work and experimental validation, receptances for different base/part are planned to be measured at location and combined with the validated machine response, thus establishing the real strength of the proposed approach in facilitating mutability and modularity.

Acknowledgements

This research was supported by the Fraunhofer Gesellschaft's ICON Project for Strategic Research Co-Operation on Sustainable Energy Technologies.
* Submitted by: Prof. Reimund Neugebauer

References

[1] L. Uriarte, M. Zatarain, D. Axinte, J. Yagüe-Fabra, S. Ihlenfeldt, J. Eguia, A. Olarra, Machine tools for large parts, Annals of CIRP, 62, (2013), pp. 731–750.

[2] R. Neugebauer, M. Wabner, H. Rentzsch, S. Ihlenfeldt, Structure principles of energy efficient machine tools, CIRP Journal of Manufacturing Science and Technology, 4, (2011), pp. 136–147.

[3] R. Bishop, D. Johnson, The mechanics of vibration, Cambridge Univ. Press, Cambridge, 1960.

[4] S.S. Park, Y. Altintas and M. Movahhedy, Receptance Coupling for end mills, International Journal of Machine Tools and Manufacture, 43, (2003), pp. 889–896.

[5] T.L. Schmitz and R. Donaldson, Predicting high-speed machining dynamics by substructure analysis, Annals of CIRP, 49, (2000), pp. 303–308.

[6] T. L. Schmitz and S. G. Duncan, Receptance coupling for dynamics prediction of assemblies with coincident neutral axes, Journal of Sound and Vibration, 289, (2006), pp. 1045–1065.

[7] G. Tuchscherer, Entwicklg. eines FEM-Modells zur Untersuchg. stat. und dyn. Eigensch. mobiler Maschinen in sich änd. Einsatzumgebungen, Diplomarbeit, TU Chemnitz, (2014)